Appl. Phys. A 78, 829–835 (2004)
DOI: 10.1007/s00339-003-2438-4

Applied Physics A
Materials Science & Processing

C. HESKE *

Spectroscopic investigation of buried interfaces and liquids with soft X-rays

Experimentelle Physik II, Universität Würzburg, Am Hubland, 97074 Würzburg, Germany

Received: 5 April 2003/Accepted: 21 October 2003
Published online: 3 February 2004 • © Springer-Verlag 2004

ABSTRACT When, in general, two entities interact, they do it by forming an interface. The properties of such interfaces are determined not only by the properties of the two interface partners, but also to a large degree by the peculiarities of the interface-formation process itself. This is of particular importance in solid-state devices composed of two or more different materials. Unfortunately, the investigation of such interfaces is very difficult for two reasons. First they are, by their nature, buried. Secondly, interfaces generally form a thin layer within a larger ensemble and thus give very weak signals. Nevertheless, a few experimental techniques are available to study such buried interfaces. This report demonstrates that a combination of soft-X-ray spectroscopies (X-ray emission, photoemission, and X-ray absorption) is extremely well suited for this task. As examples, the electronic and chemical properties of several material systems are discussed, including II–VI semiconductors, $Cu(In,Ga)(S,Se)_2$ thin-film solar cells, organic thin films, and liquids.

PACS 82.80.Ej; 73.20.-r; 68.35.Fx

1 Introduction

Understanding interfaces is one of the most multifaceted problems in experimental physics. Many of their properties – structural, electronic, physical, chemical – strongly depend on the details of the interface formation and the junction partners and are, in general, not predictable from the bulk and surface characteristics of the materials involved. Consequently, a large number of experimental techniques, e.g. X-ray diffraction and Raman scattering, have been successfully employed to assess some aspects of the interface properties, in particular in view of structural questions. Spectroscopic information about the electronic properties, in contrast, has been much more difficult to obtain. This is because the conceptually evident approach of using electron spectroscopies to study electronic properties is typically limited to information from the surface. Unless interfaces can be formed in situ, i.e. in the well-defined environment of a surface-science apparatus, electron spectroscopies can not derive information about interfaces which, by their nature, are buried.

Nevertheless, the surface sensitivity can also be put to good use in interface studies when such methods are paired with more bulk-sensitive methods. It is one of the main purposes of this report to demonstrate the analytical possibilities offered by photon-in–photon-out spectroscopy in the soft-X-ray regime (henceforth called 'X-ray emission spectroscopy' or 'resonant inelastic X-ray scattering') and its combination with electron spectroscopies. The spectroscopy with soft X-rays has had a long-standing tradition, best described in the book by Meisel et al. [1]. With the advent of third-generation synchrotron sources, previously unknown excitation flux levels and resolutions are now attainable, such that the full capabilities of these techniques, for example for studying interfaces and buried layers [2], are just now being explored to their full extent. Within this framework, we discuss some examples of the study of buried interfaces and show how a combination of X-ray emission spectroscopy with other different techniques yields information about buried interfaces, such as intermixing processes.

The paper is organized as follows: after a brief introduction to the spectroscopic methods (Sect. 2) and the experimental details (Sect. 3), an investigation of the $CdS/CuInSe_2$ thin-film solar cell heterojunction (Sect. 4.1) is discussed. This is followed by a study of humidity effects at the $ZnO/CuIn(S,Se)_2$ interface (Sect. 4.2). The third example (Sect. 4.3) discusses a study of an organic thin film and ends with an outlook on investigations of liquids, followed by a summary (Sect. 5).

2 Spectroscopic methods

Applying soft-X-ray spectroscopies to the study of interfaces and surfaces has been one of the prominent fields of surface science in the last thirty years. Photoelectron spectroscopy (PES [3]), in particular, has become the standard method to study chemical and element-specific properties of surfaces and interfaces, the latter typically in an in situ step-by-step formation of the interface (see above). As shown in Fig. 1, PES involves the ionization of a core (or valence) level and the subsequent detection of the emitted electron, with respect to both kinetic energy and angle. The short inelastic

✉ Fax: +49-931/888-5158, E-mail: heske@physik.uni-wuerzburg.de
Address after April 1, 2004: Dept. of Chemistry, University of Nevada, Las Vegas, Nevada 89154-4003, U.S.A.

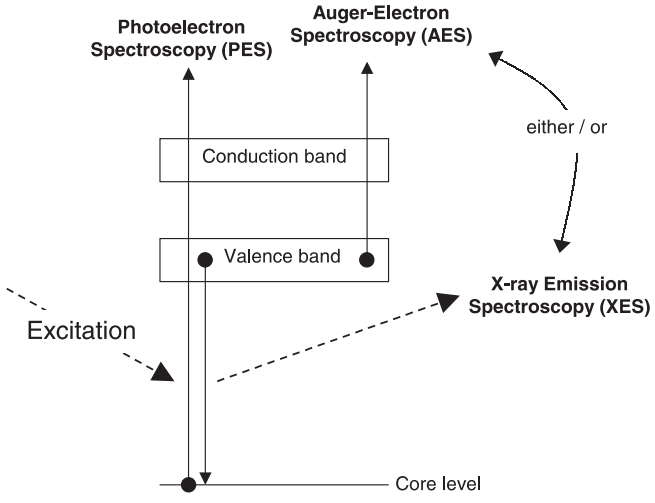

FIGURE 1 Schematic diagram of a core-level ionization (photoemission) in a semiconductor. The two competing secondary processes for filling the core hole (Auger-electron and X-ray emission) are also sketched. *Solid arrows* correspond to electrons, *dashed arrows* to photons

mean free path of the emitted electrons makes PES a surface-sensitive method (typically on the length scale of 1 nm).

A hole in an ionized core level is filled by an electron which is less strongly bound. In the present case, we particularly focus on electrons from the valence states, i.e. on electrons which are involved in the chemical bonding. As depicted in Fig. 1, there are two ways to conserve energy in the process of filling the core hole: either by emission of an Auger electron (Auger-electron spectroscopy, AES) or by emission of a fluorescence photon (X-ray emission spectroscopy, XES). While the former is also a surface-sensitive probe due to the detection of electrons, the latter is a photon-in–photon-out technique which lends itself to the study of buried systems. The attenuation length of soft X-rays in solids varies strongly as a function of photon energy and material [4] and is typically on the order of 100 nm. Hence, the near-surface bulk of a sample can be probed, and this ability is the most basic requirement for a study of buried interfaces. Furthermore, due to the localized nature of the core hole, the information derived from XES is not only atom-specific, but also from the immediate vicinity of the probed atom.

In order to obtain information about the valence states from XES spectra, the involved core level typically needs to be 'moderately shallow' (with binding energies on the order of 1000 eV or below), which requires the use of soft X-rays both on the excitation as well as on the detection side. The lifetime of such core holes is typically on the femtosecond (1–100) time scale and is most predominantly governed by the Auger decay. This means that the probability for detecting a fluorescence decay is very low; for example, in the case of the S $L_{2,3}$ XES spectra, only 0.02% of the core holes decay via fluorescence [5]. This requires a high photon flux on the excitation side and high efficiency on the detection side (in addition to a high spectral resolution), both of which are now readily available at several third-generation synchrotron sources around the world [6], but have presented a real technological challenge for the development of XES in the past.

In order to illustrate how XES can be used to identify the local chemical bonding environment, Fig. 2 (left) presents a schematic depiction of the electronic structure of CdS. By ionizing the spin–orbit-split S 2p core levels (binding energies of approximately 163 eV, angular momentum $l = 1$), we can obtain information about s- ($l = 0$) and d-like ($l = 2$) valence states such as the S 3s states and the lower valence states with strong Cd 4d contributions. Note that, due to the dipole selection rule, p-like valence states ($l = 1$) can not be observed (unless hybridized with s- or d-like states). Figure 2 (right) presents S $L_{2,3}$ XES spectra of ZnS, CdS, and HgS, and the features corresponding to the S 3s states (around 148 eV) and

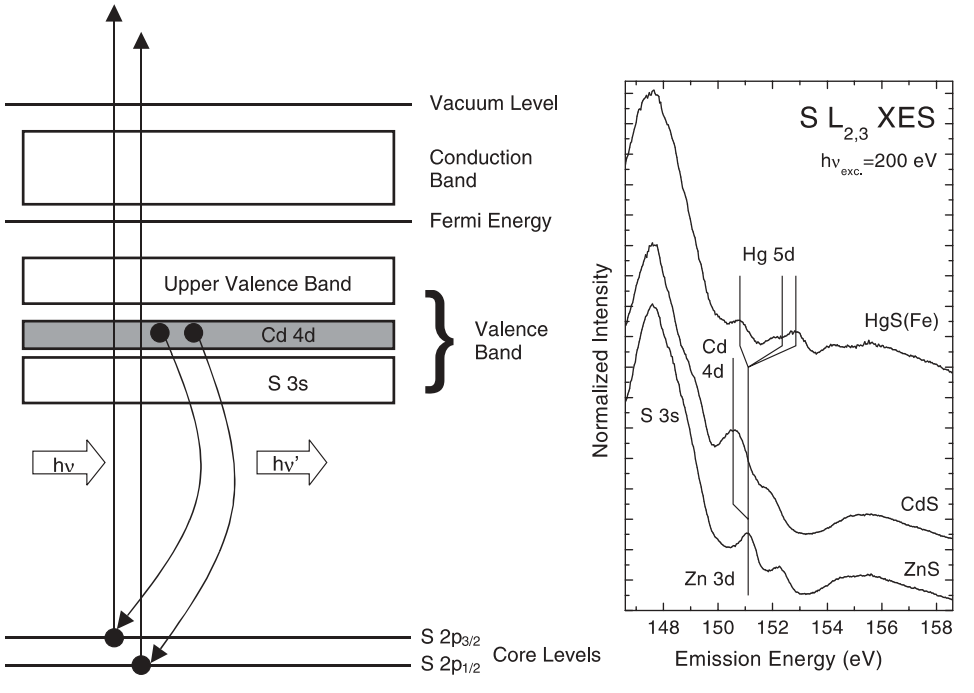

FIGURE 2 *Left*: schematic representation of the electronic structure of CdS and the processes involved in S $L_{2,3}$ XES spectra (modified from [21]). *Right*: sulfur $L_{2,3}$ spectra of ZnS, CdS, and HgS (modified from [7])

the metal d states (vertical lines) can be easily observed. Due to the creation of core holes in both the S $2p_{1/2}$ and $2p_{3/2}$ core levels, the spectra are a superposition of two individual XES spectra, separated by approximately 1.2 eV (i.e. the spin–orbit splitting of the core levels). The vertical lines give the positions of the spectral contributions due to the filling of the S $2p_{3/2}$ core hole. The presence of the metal d states in the sulfide spectra is a valuable tool, because it reveals a chemical bond between the probed sulfur atoms and the Cd atoms (for example) contributing to the lower valence band. In other words, it indicates a substantial wave-function overlap between the core hole and the delocalized valence state. Furthermore, as can be seen from Fig. 2 (right), there exist pronounced differences between the metal d states for the three different compounds. If the spectral resolution is sufficiently high, the shifts can be employed to distinguish, for example, between sulfur atoms in a ZnS and in a CdS environment [7].

Photoemission and X-ray emission processes are both initiated by non-resonant excitation, i.e. by an excitation into a continuum of final states. The corresponding pair of processes using a resonant excitation, namely X-ray absorption (XAS or NEXAFS [8]) and resonant inelastic X-ray scattering (RIXS [6]), also give a wealth of information. In the absorption process, the core electron is excited into a well-defined final state, which, near the absorption edge, is a bound but unoccupied electronic level, e.g. a conduction band of a semiconductor. Hence, amongst other things, direct information about such states can be derived (in the presence of a core hole). There are several schemes to detect the absorption process, many of which focus on detecting a secondary process due to the filling of the core hole. Among those, a variety of electron-yield (with variable surface sensitivity) and fluorescence-yield detection techniques (with 'bulk' sensitivity) are most commonly employed.

In the RIXS process, the X-ray emission after resonant excitation is recorded. This process can be viewed as an inelastic scattering process of soft X-rays, described by the Kramers–Heisenberg formalism [9], and is identical to a Raman-scattering process in which the Stokes line corresponds to an electronic excitation, e.g. of a valence electron across a band gap. Because the RIXS process is governed by energy and momentum conservation, it can be used to study the electronic bulk band structure [10]. Table 1 gives a summary of the initial and final states of photoemission, X-ray emission, and X-ray absorption spectroscopy. In all three cases, the underlying mathematical description is based on Fermi's golden rule, and in many (but by far not all [11]) cases, a dipole approximation for the relevant operator is sufficient.

	Initial state	Final state
Photoemission	Ground state	Free electron + core hole or + valence hole
X-ray emission	Core hole	Valence hole
X-ray absorption	Ground state	Excited electron + core hole
Resonant inelastic X-ray scattering	Ground state	Excited eletron + valence hole

TABLE 1 Initial and final states of several soft-X-ray spectroscopies

3 Experimental details

As mentioned above, the availability of high-flux, third-generation synchrotron sources has been an important technical development to allow the study of buried interfaces with soft X-rays, in particular using XES and RIXS. Several such sources are now available throughout the world, and consequently a number of experimental set-ups have been built to allow a routine collection of soft-X-ray spectra. The data presented here were collected at the Advanced Light Source (Berkeley), using the permanently installed soft X-ray fluorescence (SXF) end station at beamline 8.0 [12]. As for most XES spectrometers in use today (see e.g. [13]), the SXF spectrometer consists of a set of spherical gratings and an entrance slit as well as a position-sensitive detector in a Rowland-circle geometry. This geometry allows the collection of an XES spectrum in 'one shot', without any electronic or mechanical scanning, which, in principle, allows the recording of a spectrum on the time scale of seconds (if the count rate is sufficiently high). Most of the samples discussed in this report were obtained from collaboration partners as described in the original publications cited here.

4 Results

4.1 *The* CdS/ $CuInSe_2$ *thin-film solar cell heterojunction*

Solar cells on the basis of $Cu(In,Ga)(S,Se)_2$ (CIGSSe) present the most promising material system for an industrial success in the thin-film photovoltaic market. Conversion efficiencies of 19.2% for laboratory cells [14] and 12.1% for large-area modules (3651 cm^2) have been reached [15], and several companies and institutes are currently establishing pilot or production lines for large-area modules. Despite its success, the underlying physics of the CIGSSe device is definitely not sufficiently understood. In particular, the interfaces play an important role, because a typical CIGSSe device consists of several layers and interfaces; the 'standard' set-up currently consists of the following sequence: glass substrate/Mo back contact (2 μm)/CIGSSe absorber (2 μm)/CdS buffer (20–50 nm)/ZnO front contact ($\leqslant$ 2 μm). In our first example we focus on the interface of CdS on $CuInSe_2$ (CISe) [16], which is the interface responsible for the charge separation. Since the CdS buffer layer is usually deposited in a chemical bath deposition step, it is not surprising to find that the interface is by no means an ideal and abrupt heterojunction. In contrast, it is strongly intermixed, as can be learned from Fig. 3. Here, a series of S $L_{2,3}$ XES (left) and Se 3d PES (right) spectra is presented as a function of CdS film thickness. As discussed above, it is possible to directly derive information about the chemical environment of sulfur atoms from the XES spectra. In the present case, we find that the spectra for thicker CdS films agree very well with reference spectra, e.g. the CdS spectrum in Fig. 2. For very thin CdS films (5 nm), however, the S $L_{2,3}$ spectrum lacks the characteristic Cd 4d-derived peaks, which are indicative of CdS. Apparently, sulfur atoms are present, but bound in a different bonding environment, which is interpreted as a diffusion of sulfur atoms into the CISe film. In parallel, the surface-sensitive PES spectra reveal the presence of Se in the 'CdS' film, most clearly identified for the 50-nm CdS film, for which

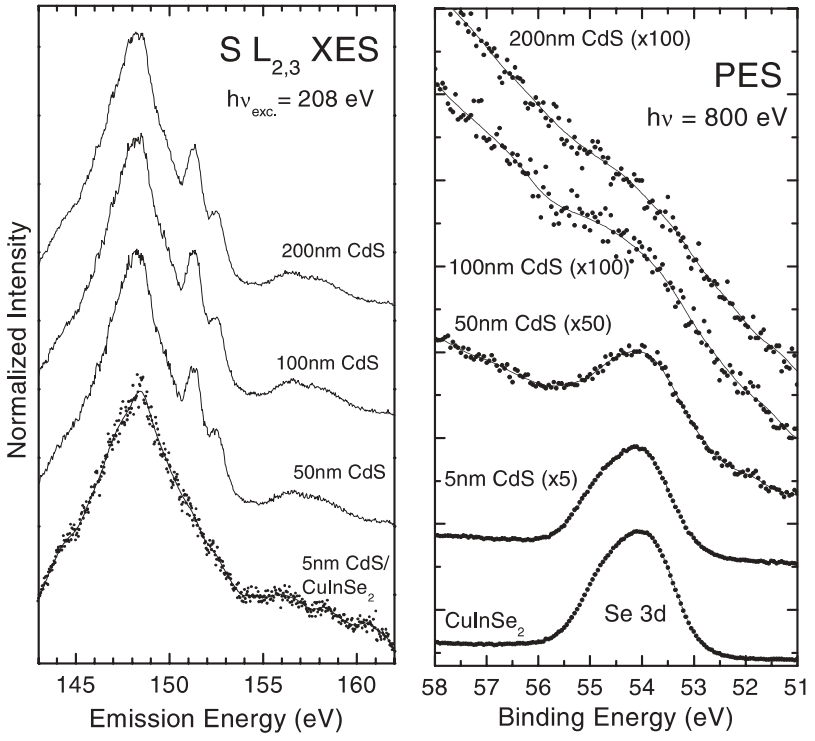

FIGURE 3 X-ray emission (*left*) and photoemission (*right*) spectra of the $CdS/CuInSe_2$ (CISe) interface formation (modified from [16])

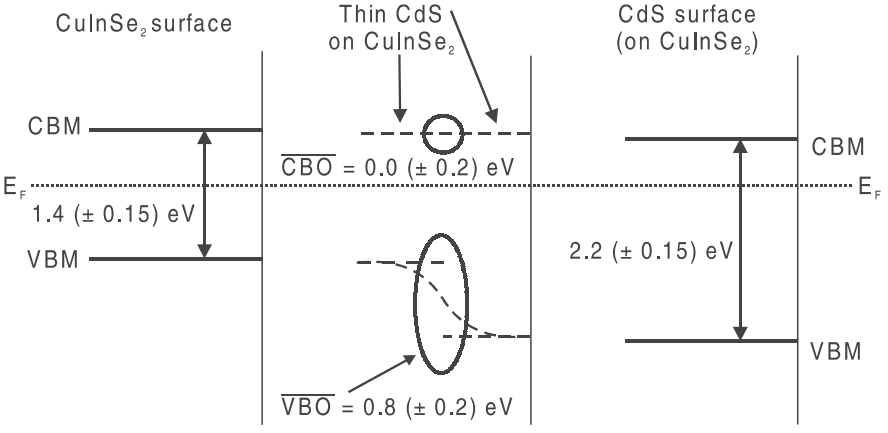

FIGURE 4 Schematic level alignment at the $CdS/CuInSe_2$ interface (from [18])

an emission from the CISe substrate can be clearly ruled out. Thus, the combination of XES and PES gives direct insight into the intermixing processes at such interfaces: while bulk-sensitive XES gives information about sulfur diffusion into the substrate, surface-sensitive PES identifies selenium atoms diffusing from the substrate into the overlayer. Interestingly, this interdiffusion process can be controlled by deliberate incorporation of sulfur atoms into the CISe surface: no Se diffusion into the CdS film is found in that case [17].

Such knowledge of interdiffusion processes is of large importance for an understanding of the CIGSSe solar cells and, in general, many other electronic devices. In the present case, the intermixing affects the band gaps of the two heterojunction partners and hence 'redesigns' the electronic level alignment at the interface. This is schematically depicted in Fig. 4, where spectroscopic data from PES and inverse PES (IPES) is summarized [18]. In IPES, the sample is excited with slow monochromatic electrons (5–20 eV) and emitted UV photons are detected. While PES gives information about the occupied valence states (in particular the valence-band maximum), IPES studies the unoccupied states (here: the conduction-band minimum). As can be seen in Fig. 4, both the band gap of the absorber surface (1.4 eV, left) and the overlayer (2.2 eV, right), are different from the expected bulk values (about 1.0 and 2.4 eV, respectively). While, in the former case, this is mostly due to a stoichiometric variation at the CISe surface [19], the latter is ascribed to the intermixing processes. Putting all data together, we find that the rearranged interface possesses a barrier-free conduction-band junction, which is favorable for electronic transport across the interface, in contrast to previously existing models within the CIGSSe community.

4.2 *Humidity effects at the* $\mathbf{ZnO/CuIn(S,Se)_2}$ *interface*

One of the central tasks for research on CIGSSe thin-film solar cells is to understand the impact of humidity on

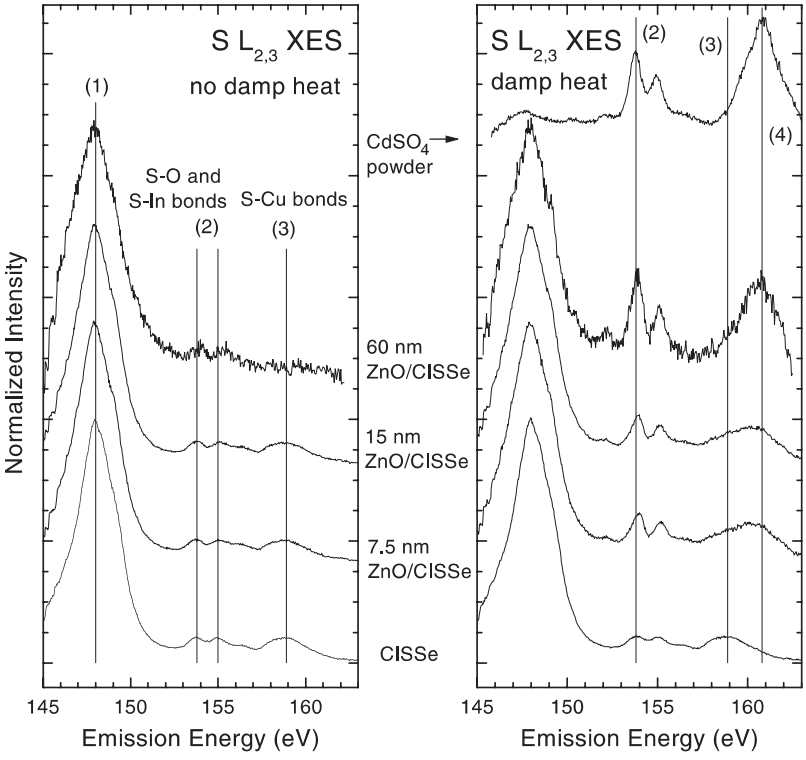

FIGURE 5 Series of S $L_{2,3}$ XES spectra of ZnO/CuIn $(S,Se)_2$ thin-film solar cell heterojunctions with varying ZnO thickness, with (*right*) and without (*left*) a damp heat treatment step (from [20])

the cell performance. This is important both from a fundamental point of view as well as for industrial applications, because of the environmental stress exerted on solar cell products. In the present case [20], we have used XES to study the impact of the so-called 'damp heat test', which consists of a 100-h storage of the cell in 80 °C, 80% humidity, and darkness. As can be seen in Fig. 5 for the ZnO/CuIn(S, Se)$_2$ interface, pronounced differences between damp heat-treated and pristine samples can be detected. The left-hand graph presents a series of ZnO films with different thicknesses (0, 7.5, 15, and 60 nm) on a CuIn(S, Se)$_2$ (CISSe) absorber. All samples were cut into two parts, and the spectra in the right-hand graph were taken with the samples after damp heat treatment. As a function of ZnO film thickness, only minor changes in the S $L_{2,3}$ XES spectra of the untreated samples can be observed. The main features of the CISSe spectrum [21], namely S 3s states in a sulfide environment (1), S 3s states indicative of S–O bonds and In 5s states indicative of S–In bonds [22] (2), and Cu 3d states indicative of S–Cu bonds (3), remain quite constant, with the exception of a reduction in peak (3) for the thickest ZnO film. In contrast, the spectrum of the treated samples show marked differences, which are easily identified as the formation of a sulfate (SO_4) by comparing with a sulfate reference spectrum (top spectrum in right-hand graph). Based on very recent experiments within the CISSY collaboration (Hahn–Meitner Institute, University of Würzburg, BESSY, and Shell Solar), employing the unique sample-scanning capabilities of the CISSY apparatus, and a study of the interface between liquid water and a CISSe absorber surface [23], this sulfate formation is possibly induced by the probing synchrotron beam. This interpretation goes beyond the description given in [21]: apparently, the well-known photochemical reaction of forming a sulfate species in a humid environment under visible light is also present when exciting with a photon energy of 200 eV. This is surprising, because, in experiments under ultra-high-vacuum conditions, the synchrotron beam has also been able to induce a decomposition of sulfate powders, forming a sulfide species. In any case, the marked difference between the two spectral series can be used to identify the presence of water at the ZnO/CISSe interface, which is of large value to understand the impact of humidity on the buried interface in more detail. This is especially important when alternative materials are employed, e.g. when the CdS layer is replaced by Zn-based II–VI semiconductors.

In summary, CIGSSe-based thin-film solar cells present a wonderful opportunity to study the chemical and electronic properties of buried interfaces with soft-X-ray spectroscopies. This is mostly due to their 'real-world' character, i.e. the fact that their interfaces are non-ideal, but rather prepared by chemically active and rather simple deposition methods which give rise to unexpected interface characteristics, such as a gradual intermixing. In particular, the large information volume of XES, in combination with other techniques such as PES and IPES, allows a spectroscopic investigation of such processes. For CIGSSe solar cells, new experimental opportunities are now available in the CISSY apparatus, which combines a large number of spectroscopic techniques (including XES and PES) with an in-system solar cell preparation at the BESSY II synchrotron-radiation source.

4.3 RIXS *of organic materials*

As mentioned above in the discussion of the spectroscopic methods, a resonant excitation can give additional information about the electronic structure of the probed material. In the case of molecules, the resonant excitation can

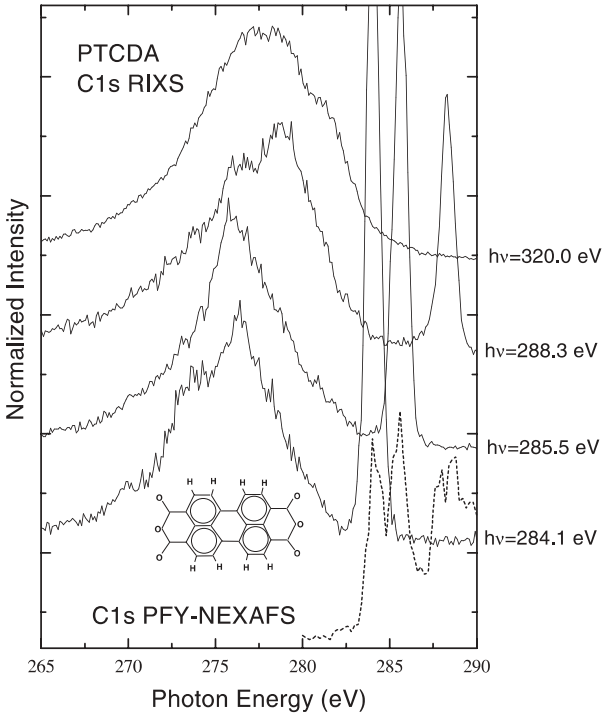

FIGURE 6 Resonant inelastic X-ray scattering (RIXS) spectra of a thick (80 nm) film of PTCDA molecules on an InSnO substrate (*top four spectra*). The *bottom* spectrum represents a partial-fluorescence-yield (PFY) X-ray absorption scan to show the positions of the π^* resonance excitations

be used to select specific sites or functional groups [24]. As an example, this is shown in Fig. 6 for the case of an 80-nm-thick PTCDA (3,4,9,10-perylene-tetracarboxylic acid-dianhydride, inset in Fig. 6) film on an InSnO (ITO) substrate. The bottom spectrum (dotted line) gives a coarse partial fluorescence yield X-ray absorption spectrum (PFY-NEXAFS) at the C K edge. Note that the low spectral quality of this spectrum is due to the detection with the RIXS detector, which gives good spectral resolution on the detection side but rather low count rates. Here it is merely shown to allow a direct comparison with the excitation energies of the RIXS spectra to be discussed below. Based on a detailed analysis of PTCDA NEXAFS spectra [25], it is known that the lowest two π^* resonances of the K-edge spectrum (284.1 and 285.5 eV) mostly correspond to the carbon atoms within the perylene ring system, while excitation at 288.3 eV predominantly excites carbon atoms of the anhydride groups.

The upper four spectra in Fig. 6 represent a series of RIXS spectra as a function of excitation energy (given on the right-hand side). The uppermost spectrum corresponds to a non-resonant excitation (i.e. the XES case), while the other three spectra were excited at the energies (i.e. NEXAFS peaks) discussed above. Clearly, the elastically scattered peak (the Rayleigh line) can be observed in the three resonant spectra, and they coincide nicely with the positions of the corresponding π^* resonances in the NEXAFS spectrum. The observed RIXS spectra vary strongly between the different excitation energies, in particular between excitations in the perylene ring system and at the anhydride groups. These differences are ascribed to a spatially varying distribution of the occupied molecular orbitals (and their wave-function

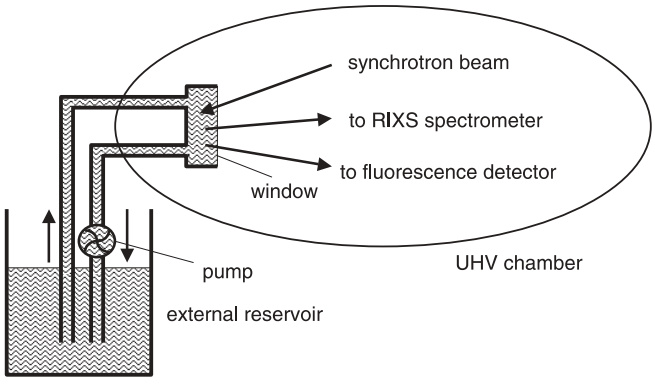

FIGURE 7 Schematic diagram of an in situ wet-cell apparatus for soft-X-ray spectroscopies currently under construction

overlap with the respective core hole) within the different regions of the molecule. Detailed calculations on the basis of the Kramers–Heisenberg formalism are currently under way to elucidate the detailed excitation-energy dependence of the RIXS spectra.

Due to the resonant excitation, in some cases into antibonding orbitals, molecular decomposition processes can also play an important role when taking RIXS spectra of organic molecules. This requires an optimization of the experimental set-up in order to minimize the impact of such effects. First, the sample should be continuously scanned while taking such data, which requires very accurate and stable motorization. Secondly, exposure times should be minimized by optimizing the efficiency of the RIXS spectrometer; a number of different alternative designs is currently under construction. Finally, individual molecules (or clusters) can be studied in a flow-through mode, either in gas phase or in solution. The latter case is depicted in Fig. 7, where a flow-through liquid cell for RIXS and NEXAFS studies is schematically depicted. At present, 'static' liquid cells have already been successfully used to study liquid water [26] and liquid/solid interfaces [23]. Apart from the study of molecular solutions, the properties of water itself are an intense field of research, and soft-X-ray spectroscopies have already shown a lot of promise in learning about the intricate details of the hydrogen-bonding network [27].

5 Summary and outlook

Soft-X-ray spectroscopies offer a wealth of information about the electronic structure of buried interfaces and liquids. This has already been true for the last thirty years, but the experimental possibilities offered at third-generation synchrotron sources have now added a new dimension of analytical and experimental opportunities. In particular, X-ray emission spectroscopy and resonant inelastic X-ray scattering have become readily available, and the exploration of the additional information channels offered by these tools is currently in full progress. As discussed in this report, combining different soft-X-ray techniques is particularly valuable. In the study of interfaces, for example, the combination of surface- and bulk-sensitive techniques allows a more complete understanding of intermixing processes and intermediate phase formations, even if the in-

terfaces are buried. This is of large importance for many industrially relevant preparation methods, in which no well-defined interfaces are formed. Therefore, this area of research presents an interesting mixture: it comprises the drive to understand fundamental questions, the need for technological development of experimental set-ups, and the solution of applied issues in optimizing the electronic and chemical structure of electronic devices with buried interfaces and layers.

ACKNOWLEDGEMENTS The author is very grateful to the following individuals for their collaboration, help, and support: U. Groh, L. Weinhardt, O. Fuchs, D. Eich, M. Morkel, L. Chkoda, R. Fink, and E. Umbach (Experimentelle Physik II, Universität Würzburg), F. Karg and his team from Shell Solar, München (formerly Siemens Solar GmbH), C.-H. Fischer, M.-C. Lux-Steiner, and the CISSY team (Hahn–Meitner Institute, Berlin), Y. Zubavichus and M. Grunze (Universität Heidelberg), M. Grün and C. Klingshirn (Universität Karlsruhe), W. Szuszkiewicz (Polish Academy of Sciences, Warsaw), C. Bostedt and L.J. Terminello (Lawrence Livermore National Laboratory), and J.D. Denlinger (Advanced Light Source, Berkeley). This work was supported by the German BMWI (FKZ 0329218C) and BMBF (FKZ 05KS1WW1/6) and the Deutsche Forschungsgemeinschaft through SFB 410, TP B3.

REFERENCES

1 A. Meisel, G. Leonhardt, R. Szargan: *X-Ray Spectra and Chemical Binding* (Springer Ser. Chem. Phys. **37**) (Springer, Berlin, Heidelberg 1989)
2 J.A. Carlisle, L.J. Terminello, E.A. Hudson, R.C.C. Perera, J.H. Underwood, T.A. Callcott, J.J. Jia, D.L. Ederer, F.J. Himpsel, M.G. Samant: Appl. Phys. Lett. **67**, 34 (1995)
3 S. Hüfner: *Photoelectron Spectroscopy* (Springer Ser. Solid-State Sci. **82**) (Springer, Berlin, Heidelberg 1995)
4 http://www-cxro.lbl.gov/optical_constants, Center for X-ray Optics, Lawrence Berkeley National Laboratory, Berkeley, CA 94 720, USA
5 M.O. Krause: J. Phys. Chem. Ref. Data **8**, 307 (1979)
6 See various articles in J. Electron Spectrosc. Relat. Phenom. **110–111** (2000)
7 C. Heske, U. Groh, O. Fuchs, L. Weinhardt, E. Umbach, M. Grün, S. Petillon, A. Dinger, C. Klingshirn, W. Szuszkiewicz, A. Fleszar: Appl. Phys. Lett. **83**, 2360 (2003)
8 J. Stöhr: *NEXAFS Spectroscopy* (Springer Ser. Surf. Sci.) (Springer, Heidelberg, Berlin 1992)
9 Y. Ma: Phys. Rev. B **49**, 5799 (1994)
10 S. Eisebitt, W. Eberhardt: J. Electron Spectrosc. Relat. Phenom. **110–111**, 335 (2000), and references therein
11 O. Hemmers, G. Fisher, P. Glans, D.L. Hansen, H. Wang, S.B. Whitfield, D.W. Lindle, R. Wehlitz, J.C. Levin, I.A. Sellin, R.C.C. Perera, E.W.B. Dias, H.S. Chakraborty, P.C. Deshmukh, S.T. Manson: J. Phys. B **30**, L727 (1997)
12 J.J. Jia, T.A. Callcott, J. Yurkas, A.W. Ellis, F.J. Himpsel, M.G. Samant, J. Stöhr, D.L. Ederer, J.A. Carlisle, E.A. Hudson, L.J. Terminello, D.K. Shuh, R.C.C. Perera: Rev. Sci. Instrum. **66**, 1394 (1995)
13 J. Nordgren, J. Guo: J. Electron Spectrosc. Relat. Phenom. **110–111**, 1 (2000)
14 K. Ramanathan, M.A. Contreras, C.L. Perkins, S. Asher, F.S. Hasoon, J. Keane, D. Young, M. Romero, W. Metzger, R. Noufi, J. Ward, A. Duda: Prog. Photovolt.: Res. Appl. **11**, 225 (2003)
15 M.A. Green, K. Emery, D.L. King, S. Igari, W. Warta: *Solar Cell Efficiency Tables* (ver. 22), Prog. Photovolt.: Res. Appl. **11**, 347 (2003)
16 C. Heske, D. Eich, R. Fink, E. Umbach, T. van Buuren, C. Bostedt, L.J. Terminello, S. Kakar, M.M. Grush, T.A. Callcott, F.J. Himpsel, D.L. Ederer, R.C.C. Perera, W. Riedl, F. Karg: Appl. Phys. Lett. **74**, 1451 (1999)
17 L. Weinhardt, M. Morkel, T. Gleim, S. Zweigart, T.P. Niesen, F. Karg, C. Heske, E. Umbach: in *Proc. 17th Eur. Photovoltaic Solar Energy Conf., Munich, October 2001*, p. 1261
18 M. Morkel, L. Weinhardt, B. Lohmüller, C. Heske, E. Umbach, W. Riedl, S. Zweigart, F. Karg: Appl. Phys. Lett. **79**, 4482 (2001)
19 D. Schmid, M. Ruckh, F. Grunwald, H.W. Schock: J. Appl. Phys. **73**, 2902 (1993); D. Schmid, M. Ruckh, H.W. Schock: Sol. Energy Mater. Sol. Cells **41**, 281 (1996)
20 C. Heske, U. Groh, L. Weinhardt, O. Fuchs, B. Holder, E. Umbach, C. Bostedt, L.J. Terminello, S. Zweigart, T.P. Niesen, F. Karg: Appl. Phys. Lett. **81**, 4550 (2002)
21 C. Heske, U. Groh, O. Fuchs, E. Umbach, N. Franco, C. Bostedt, L.J. Terminello, R.C.C. Perera, K.H. Hallmeier, A. Preobrajenski, R. Szargan, S. Zweigart, W. Riedl, F. Karg, Phys. Status Solidi A **187**, 13 (2001)
22 R.S. Crisp, D. Haneman, J.W. Chu: Solid State Commun. **83**, 1035 (1992)
23 C. Heske, U. Groh, O. Fuchs, E. Umbach, T. Schedel-Niedrig, C.-H. Fischer, M.Ch. Lux-Steiner, S. Zweigart, F. Karg, J.D. Denlinger, B. Rude, C. Andrus, F. Powell: J. Chem. Phys. **119**, 10 467 (2003)
24 A. Nilsson, M. Weinelt, T. Wiell, P. Bennich, O. Karis, N. Wassdahl, J. Stöhr, M.G. Samant: Phys. Rev. Lett. **78**, 2847 (1997); A. Nilsson: J. Electron Spectrosc. Relat. Phenom. **126**, 3 (2002)
25 J. Taborski, P. Väterlein, H. Dietz, U. Zimmermann, E. Umbach: J. Electron Spectrosc. Relat. Phenom. **75**, 129 (1995)
26 J.-H. Guo, Y. Luo, A. Augustsson, J.-E. Rubensson, C. Såthe, H. Ågren, H. Siegbahn, J. Nordgren: Phys. Rev. Lett. **89**, 137 402 (2002)
27 S. Myneni, Y. Luo, L.A. Näslund, M. Cavalleri, L. Ojamäe, H. Ogasawara, A. Pelmenschikov, Ph. Wernet, P. Väterlein, C. Heske, Z. Hussain, L.G.M. Pettersson, A. Nilsson: J. Phys.: Condens. Matter **14**, L213 (2002) and references therein